Multigrid deconvolution of seismic data

John Millar and John C. Bancroft

ABSTRACT

A multigrid method for deconvolution is developed. Tests on synthetic seismic data show the method to be stable, and convergent, and comparisons to a time-domain Gauss-Seidel iterative approach are made to emphasize the long wavelength correction properties of multigrid. The main advantage to the time-domain methods outlined is a straightforward extension to using a nonstationary wavelet. As well, a method for imaging reflectors in-between sample points was found. This may be achieved by interpolating the data to a higher resolution, prior to a multigrid deconvolution.

INTRODUCTION

Multigrid methods are an efficient and robust group of algorithms, used for the solution of large linear and non-linear systems of equations. The purpose of our study was to apply a multigrid-style solver to the deconvolution problem, and study the effects of interpolation, restriction, and Gauss-Seidel relaxation on seismic data. For an introduction to multigrid methods, see Millar and Bancroft (2003).

Multigrid methods work by applying an antialias filter to the data, then rejecting samples to reduce the number of grid points. Once a solution is found on the coarse grid, it is interpolated to a finer grid spacing and corrected using an iterative method such as the Gauss-Seidel relaxation. This interpolation and correction is repeated until the desired mesh spacing and accuracy are achieved.

The reason for the success of multigrid is two-fold. For one, a large part of the computation is performed on a smaller system of equations. For most of the calculation, there are less points to calculate. Secondly, with the right choice of correction method, the error reducing capabilities are focussed on the error introduced by the interpolation step.

The power of multigrid is demonstrated in the following figures. Figure 1(a) shows the error of an initial estimate to the solution of Laplaces equation. Figures 1(b), 1(c) and 1(d) show the error after 3, 10, and 30 iterations of the Gauss-Seidel relaxation, respectively. The high-frequency component of the error is reduced very quickly, however the long wavelength error remains after many iterations of the correction.

The coarse grid correction process, one of many multigrid schemes, is demonstrated in Figure 2. The initial estimate (displayed again in 2(a)) to our sample problem was restricted to a sampling interval 8 times larger than the original. The restricted solution is shown in 2(b). From there, only 3 iterations of the Gauss-Seidel relaxation were performed, yielding the result in 2(c). The result was then interpolated to the original sampling interval in 2(d). The number of computer operations is approximately equal to just one iteration of the Gauss-Seidel correction at full resolution. Were the restriction to continue to a coarser grid, it would take even less effort to reduce the error to zero.

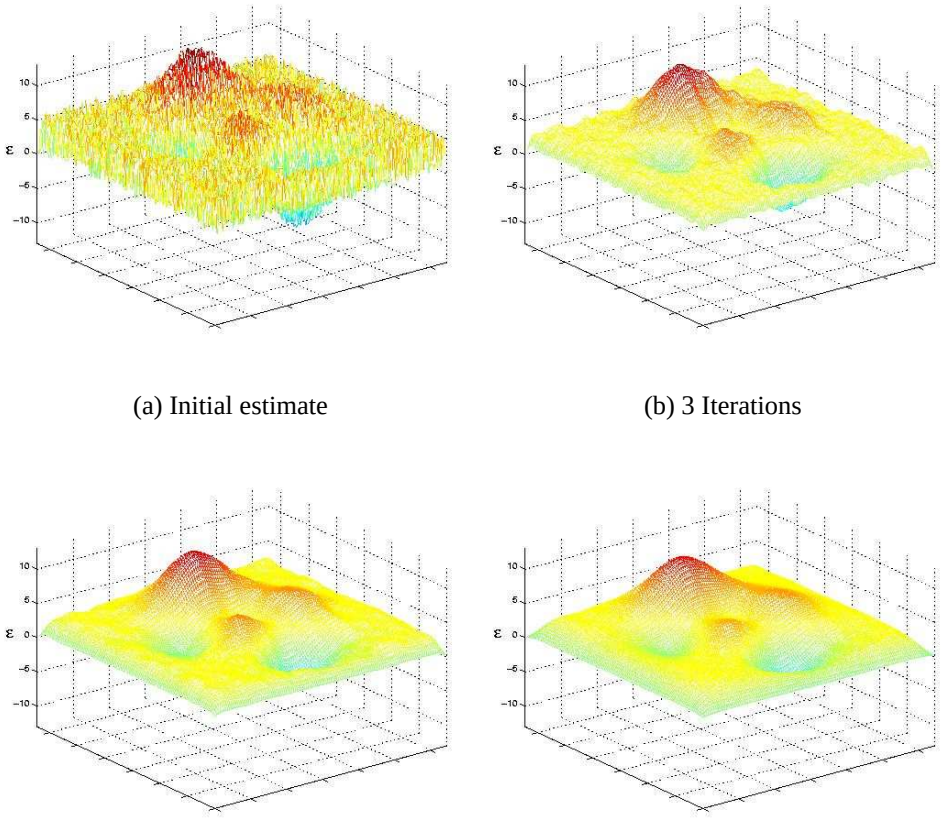

(a) Initial estimate (b) 3 Iterations

(c) 10 Iterations (d) 30 Iterations

FIG. 1. Successive Gauss-Seidel iterations to find a solution to Laplace's Equation. Vertical axes show error, (ϵ).

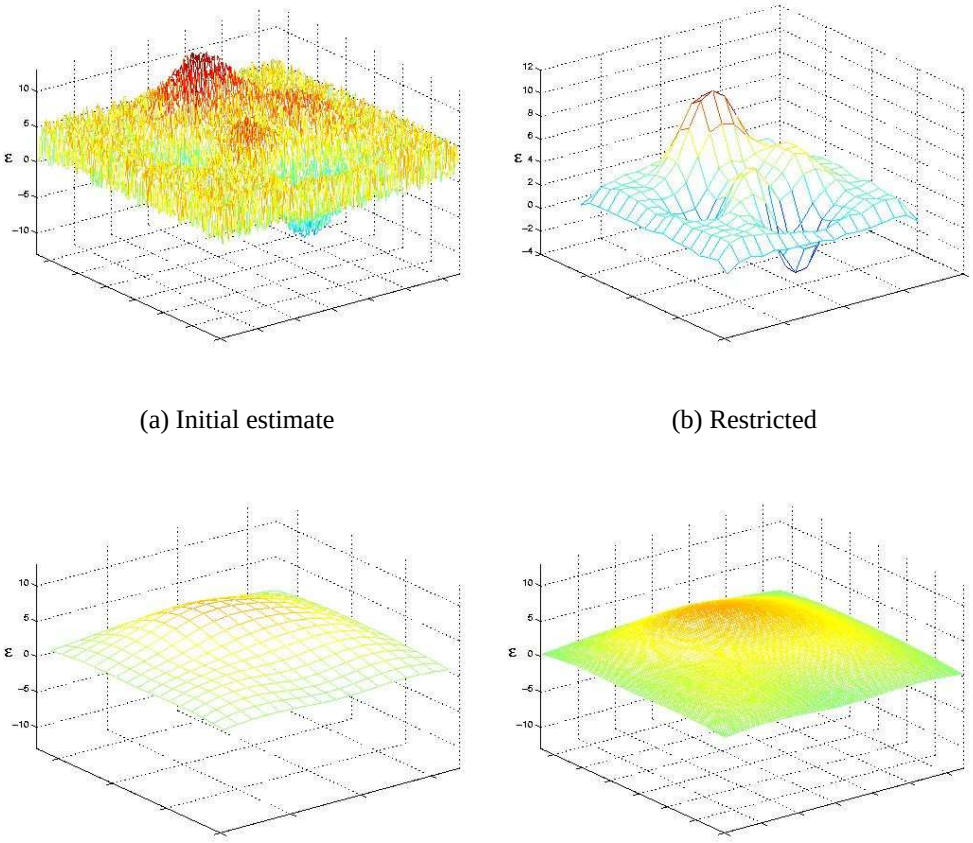

(a) Initial estimate

(b) Restricted

(c) Corrected on coarse grid

(d) Interpolated

FIG. 2. Effect of Gauss-Seidel correction on a coarse grid. Vertical axes show error, (ϵ).

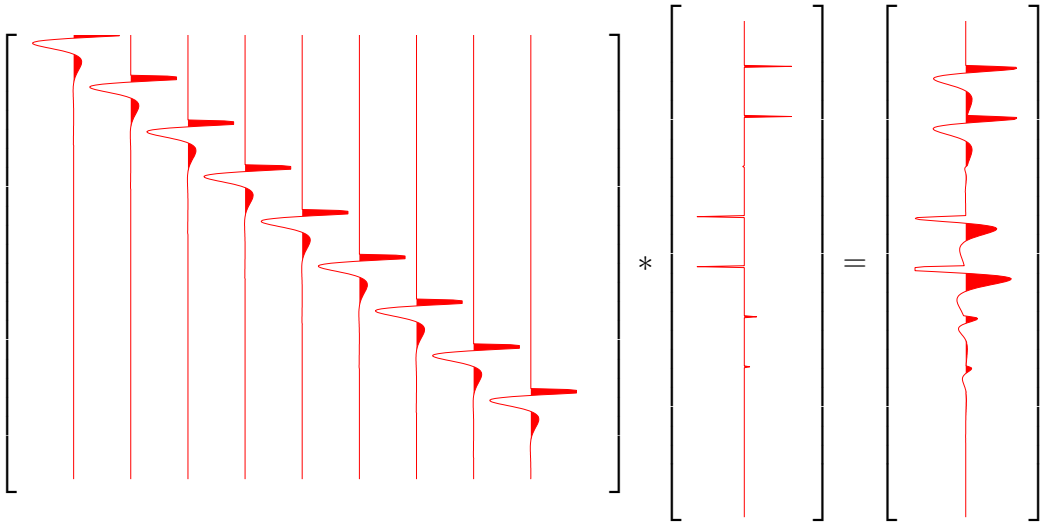

FIG. 3. The convolutional model as a matrix multiplication.

GAUSS-SEIDEL DECONVOLUTION

We express the convolutional model as a system of linear equations,

$$\mathbf{Wr} = \mathbf{s}. \tag{1}$$

The vector $\mathbf{r}$ is the reflectivity series, and $\mathbf{s}$ is the recorded seismic trace. Each column of the matrix $\mathbf{W}$ is the seismic wavelet, with time zero (t_0) of the wavelet lying on the main diagonal. The expression of a convolution as a matrix operation is diagrammed in Figure 1.

For the Gauss-Seidel algorithm to work, it requires a diagonally dominant system (Trottenberg et al., 2001). In order to ensure that this is the case, we use instead

$$\mathbf{W^T W r} = \mathbf{W^T s}, \tag{2}$$

where the superscripted T denotes the transpose.

To derive the Gauss-Seidel correction for this system of N equations , we inspect the i^{th} equation,

$$\sum_j [\mathbf{W^T W}](i,j)\mathbf{r}(j) = [\mathbf{W^T s}](i), \qquad j = 1, N. \tag{3}$$

Solving (3) for $r(i)$,

$$\frac{\sum_{\mathbf{j}}[\mathbf{W^T W}](i,j)\mathbf{r}(j) - [\mathbf{W^T s}](i)}{[\mathbf{W^T W}](i,i)} = \mathbf{r}(i), \qquad j = 1, N, \quad j \neq i. \tag{4}$$

To apply this correction, we cycle through the entire trace, updating each sample in the trace with Equation 4. Results are far superior if the direction of the cycle changes with each iteration; *i.e.*, the first iteration starts at time zero and moves down the trace, the second iteration starts at maximum time and moves up the trace.

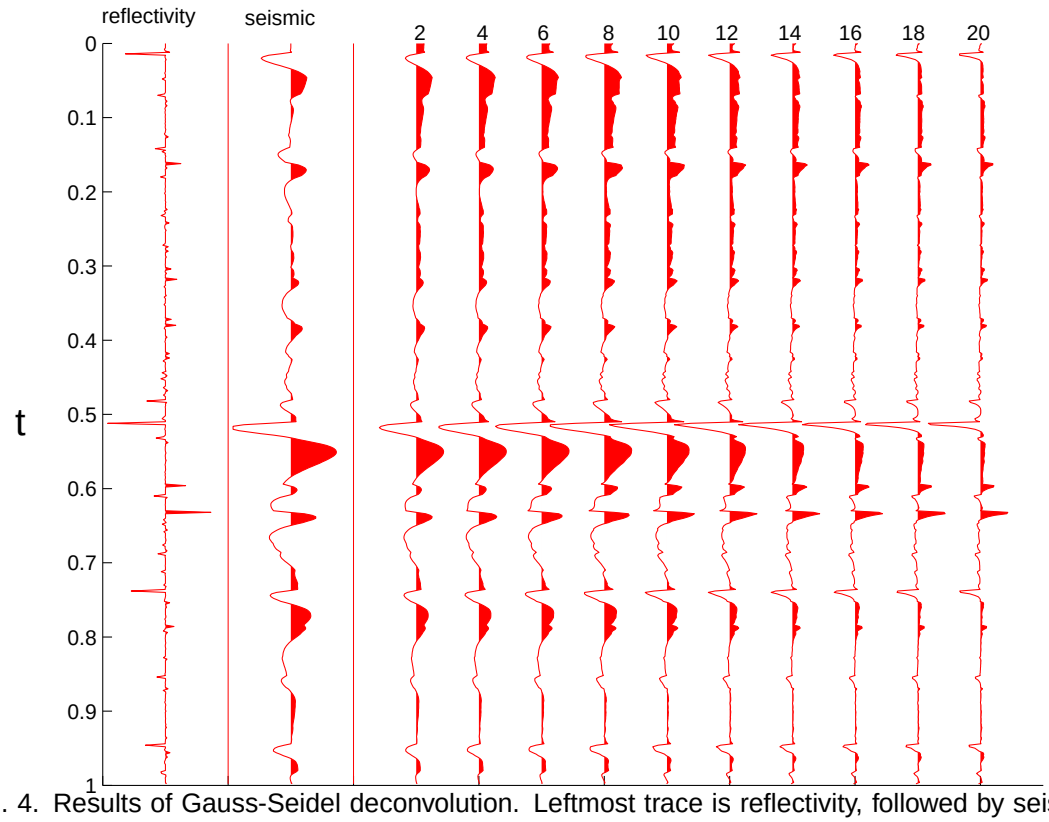

FIG. 4. Results of Gauss-Seidel deconvolution. Leftmost trace is reflectivity, followed by seismic, then progressive iterations of the correction to the right, with the number of iterations at the top of the trace.

The results of the Gauss-Seidel deconvolution are satisfactory. In the case of an exact known wavelet, with frequency right up to the Nyquist frequency, the deconvolution recovers the reflectivity series exactly. As is predicted, in Figure 4, the high-frequency component of the reflectivity is resolved quite quickly, while the lower-frequency errors tend to be more difficult to reduce, taking many iterations for an improvement in the solution.

MULTIGRID DECONVOLUTION

For the multigrid deconvolution, a coarse grid correction approach was used. The seismic data and the wavelet were antialias-filtered and reduced to a sample rate 8 times that of the original. This restricted wavelet was used to perform a Gauss-Seidel correction on the trace. The solution was interpolated, and corrected again. Alternating interpolations and corrections were made until the trace was returned to the original sample rate. Several iterations of the coarse grid correction were made. The results are shown in Figure 5, showing how the solution is refined after each interpolation. Trace 1 is the seismic data reduced to 8 times the sample rate. Traces 2-4 show the trace after each interpolation and correction pair. The remaining traces show the result after progressive iterations of the coarse grid correction. As predicted, at the coarser grid spacing the long-wavelength errors are removed very quickly. The last seven traces are successive passes of the correction at the fine grid spacing, however very little improvement is made after the first pass. The high

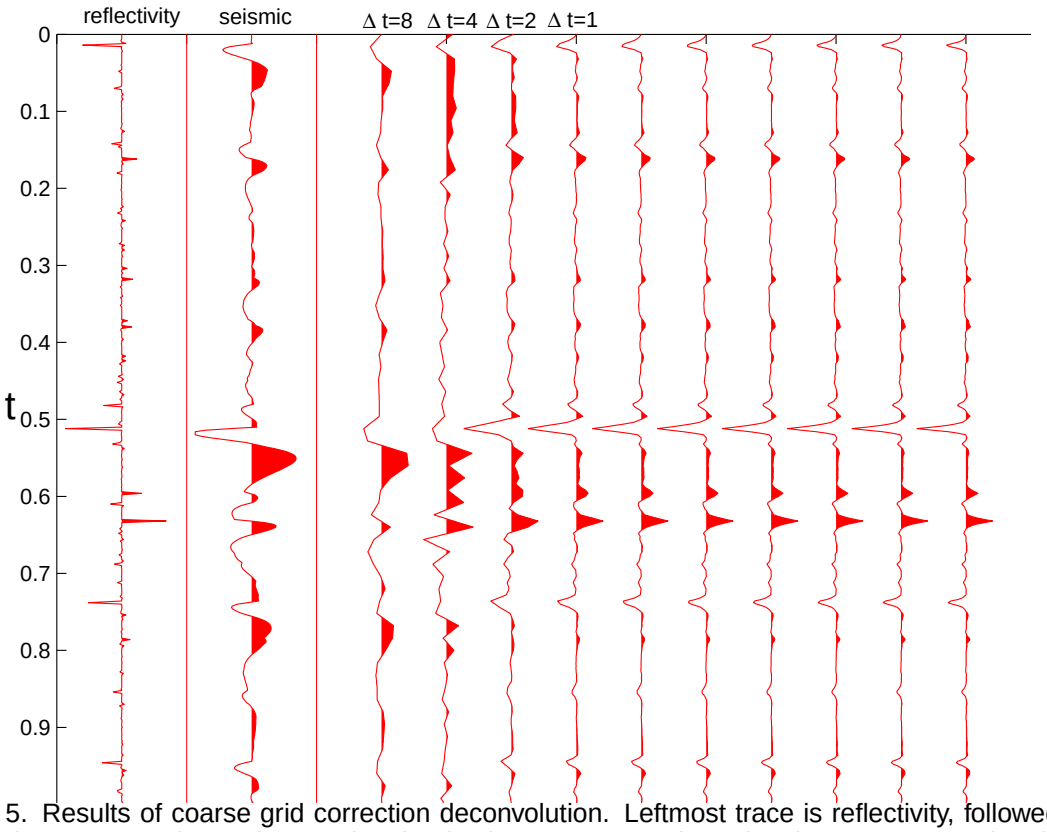

FIG. 5. Results of coarse grid correction deconvolution. Leftmost trace is reflectivity, followed by seismic. Trace 1 shows the restricted seismic, Traces 2-4 show the data at 8, 4, and 2 times sampling intervals, after the correction. Traces 5-10 show solution after successive coarse grid corrections.

frequencies are not well resolved.

To take advantage of both methods, a single pass of the coarse grid correction was made to estimate the long wavelengths, followed by successive passes of the Gauss-Seidel algorithm to correct the higher frequencies. It can be seen in Figure 6 that this method yields results faster than the Gauss-Seidel method alone, and has the higher frequency components converging.

RESOLUTION EXPERIMENT

A numerical experiment was performed, where a reflectivity spike was placed in-between samples in time, to see if interpolation past the original sampling interval would resolve the reflectivity location. The original seismic trace was calculated at 0.1ms sampling interval. The data was then re-sampled at a 2 ms interval, without any antialias-filtering applied. The reflectivity spike was set in-between two samples of the 2 ms data. The Gauss-Seidel method was unable to resolve the point. The Weiner frequency domain deconvolution produced aliasing. The multigrid data was able to roughly place the reflector in-between the samples. While the method was unable to introduce any new frequency content to the data, it does seem that the method is able to correct the phase adequately to place the reflector properly.

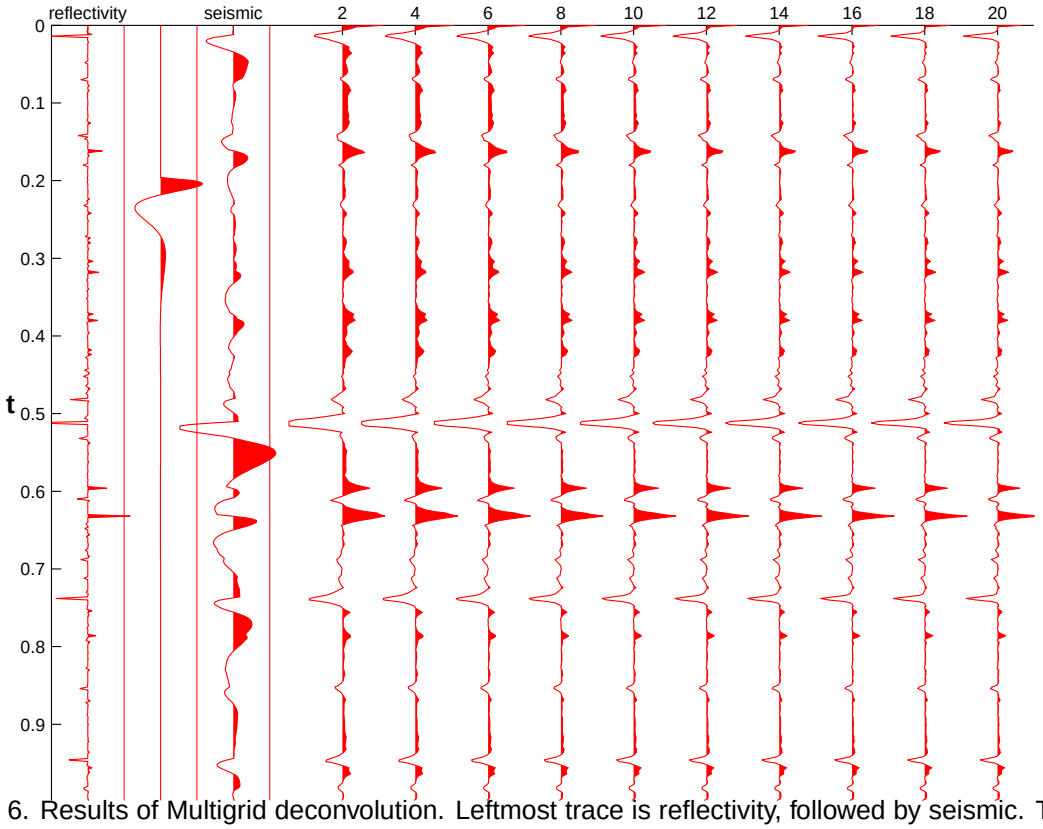

FIG. 6. Results of Multigrid deconvolution. Leftmost trace is reflectivity, followed by seismic. Trace 1 shows the coarse grid corrected reflectivity, followed by successive Gauss-Seidel corrections at full resolution.

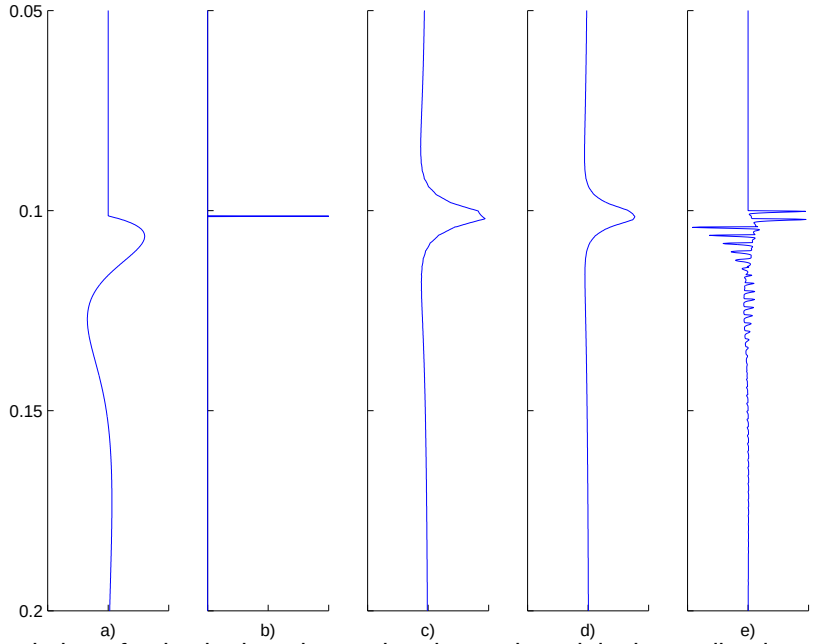

FIG. 7. Deconvolution of seismic data, interpolated past the original sampling interval: a) Seismic; b) Reflectivity; c) Gauss-Seidel deconvolution result; d) Multigrid Deconvolution; e) Weiner frequency domain deconvolution.

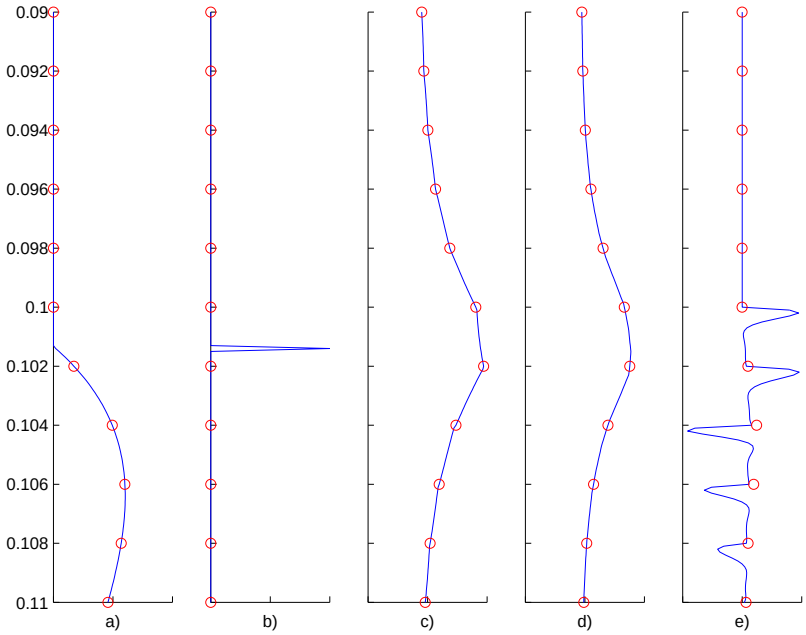

FIG. 8. Deconvolution of seismic data, interpolated past the original sampling interval: a) Seismic data, blue 0.1 ms sample interval, red dot 2 ms sample interval; b) Reflectivity; c) Gauss-Seidel deconvolution result; d) Multigrid Deconvolution; e) Weiner frequency domain deconvolution.

CONCLUSIONS

Results show that multigrid methods are an effective way to deconvolve seismic data. The quality of the deconvolution rests on both the ability to estimate the wavelet and the frequency content. The usefulness of the method will rely heavily on the ability to quickly estimate the embedded wavelet. Tests comparing the relative speed of multigrid to other deconvolution algorithms have not been conducted.

One strength of the method that has not been explored in this paper is the ease with which a nonstationary wavelet could be used. The modifications to the code is minor, and the run time will not be affected greatly.

The multigrid deconvolution algorithm also provides a method to resolve a reflectivity in between samples. This may be of use in determining to a greater accuracy the thickness and depth of thin beds.

REFERENCES

Millar, J., and Bancroft, J. C., 2003, Multi-grid principles: CREWES Research Report, **15**.

Press, W. H., Teukolsky, S. A., Vetterling, W. T., and Flannery, B. P., 1992, Numerical Recipes in C, 2nd edn: Cambridge University Press.

Shewchuk, J. R., 2002, An Introduction to the Conjugate Gradient Method Without the Agonizing Pain: unpublished.

Shih, R. C., and Levander, A. R., 1985, Multi-grid reverse-time migration: American Geophysical Union, fall meeting.

Trefethen, L. N., 1996, Finite Difference and Spectral Methods for Ordinary and Partial Differential Equations: unpublished.

Trottenberg, U., Oosterlee, C., and Schűller, A., 2001, Multigrid: Academic Press.

Wesseling, P., 1992, An Introduction to Multigrid Methods: John Wiley & Sons.